Chapter 6

Transport of Electrolyte in Organic Coatings on Metal

Zoi Manoli, Darja Pecko, Guy Van Assche,
Johan Stiens, Ali Pourkazemi and Herman Terryn

Additional information is available at the end of the chapter

http://dx.doi.org/10.5772/intechopen.81422

Abstract

Organic coatings form an effective barrier between metals and their environment, providing them protection against corrosion. Corrosion on coated metals depends mainly on the diffusion of water through the coating, the loss of adhesion at the interface between the coating and the metal (delamination), the rate of the chemical and electrochemical reactions under the coating and the treatment of the metal surface before the coating application. Many aggressive ions are transported toward and inside the coating through water. In organic coatings, typically, the water absorbed by the coating affects the polymer matrix structure, and it causes swelling and stresses, which may result in cracks. Swelling and cracks enhance the transport of water into the solid polymer, and concurrently the diffusion of ions. Over time also, the chemical structure of the polymer may change, adversely affecting its barrier properties and overall performance. In this chapter, we focus on methods to quantify the transport of electrolyte in organic coatings. We mark out the main characteristics, advantages and limitations of each one of them.

Keywords: water uptake, organic coating, corrosion, gravimetric method, ATR-FTIR, NMR, THz-TDS, THz-FDS, EIS

1. Introduction

Organic coatings are used to protect metals against corrosion. In transportation, infrastructure, and oil and gas industry, just to name a few, corrosion has not only a serious economic impact (productivity and efficiency reduction), but it also harms the environment and reduces public safety. Therefore, coatings are extensively used to slow down the degradation of metals, thus extending the service lifetime of structures. An organic corrosion-protection coating applied on a metallic surface forms a barrier between the metal surface and its environment, preventing or delaying the transportation of corrosive species toward the metal, thus retarding the creation

of rust at the metal surface. Over time, also the coating will degrade, reducing its barrier properties and corrosion protection efficiency. Scratches in the coating, pinholes, and surface contamination in between the coating and the metal are the main factors of coating degradation [1, 2]. Mechanical damages can be the pathways for enhanced water diffusion. The long-term performance of polymeric coatings highly depends on water adsorption and absorption. Typically, the polymer absorbs water, which affects the structure of the polymer matrix, causing swelling and internal stresses, thus producing nanosized channels and even cracks, enhancing the transport of water into the solid polymer and thus reducing its barrier properties. Additionally, the sorption of water may affect the polymer's mechanical properties by acting as a plasticizer and, in some cases, by causing hydrolysis. Progressively, the polymer degrades, losing its mechanical performance. The higher the temperature in a humid environment and the longer the time, the faster the polymer's degradation takes place. By calculating the amount of water that ingresses into the coating, and the diffusion coefficient, it is feasible to estimate the starting point in time where the corrosion may start occurring on the metal surface. After that point, the deterioration of the coating-metal interface begins. Given such parameters (amount and diffusion coefficient of water) it is feasible to optimize the quality of the coating (components, structure and thickness) in order to slow the process of corrosion down. The water uptake by coatings has been investigated by many researchers. However, most of the experimental techniques used, work under ideal and stable conditions, i.e. coatings without pinholes, scratches or any kind of defects, constant temperatures and humidity. The reason is that a combination of different physical and chemical phenomena can occur simultaneously; hence, different parameters affect the water uptake phenomena. The most common techniques to study water uptake in coatings are gravimetric method (GM), attenuated total reflection Fourier transform infrared spectroscopy (ATR-FTIR) and nuclear magnetic resonance (NMR). The amount of water sorpted can also be estimated using electrochemical techniques, such as electrochemical impedance spectroscopy (EIS). A novel, non-destructive evaluation for water penetration is provided by terahertz spectroscopy. Nevertheless, these techniques give reliable results given that they deal with ideal organic coatings (no defects, homogeneous surface) so as to consider only the diffusion phenomenon. In this chapter, we will first discuss the transport of water and electrolyte into organic coatings. Subsequently the experimental techniques for studying these processes will be looked at.

2. Organic coatings: barrier to electrolyte entrance

Organic coatings are thin solid-phase materials, which can be applied on structures to provide corrosion protection, and provide many other functions, such as, mechanical and chemical protection, electrical and thermal conductivity isolation, hydrophilicity or hydrophobicity, UV resistance, or esthetic properties, such as color, gloss or roughness [3, 4]. The formulation used to apply an organic coating typically consists of a binder and fillers, and in some case solvents or water (e.g., in latex paints). The compatibility of the components and their volume fraction, as well as the number of coating layers that are applied on a substrate, affects the properties and the functionality that the coating will finally reach. According to Szauer [5], an improper

dispersion of molecules may leave free spaces available to be covered by corrosive species [6]. Despite development in coating technologies, troubles in corrosion protection of metals continue to exist in the long run. Substantial research has been done to understand scientifically the modes of failure of these materials in particular environmental conditions. Nevertheless, there has been limited work to quantitatively mark out the deterioration process and to predict the lifetime of the coated metal. One of the main reasons is the complexity of the coating/metal system and the combination of factors that simultaneously affect the performance of the coating. This encompasses the physical and chemical properties of the polymer, the substrate surface, the interface between coating and metal, the presence of defects, or local inhomogeneities. For example, low-molecular-weight or low-crosslinked materials can take up a large amount of water, and may show a low resistance to ion transport, hence they are susceptible to water attack. Corrosion takes place at the defects (pinholes, pores, scratches) and delamination or blisters appear adjacent to them.

When the coated metal is exposed to an aqueous solution, the water immediately starts spreading through the organic matrix. As for ion diffusion, most coatings work as a barrier due to their low dielectric constants and the limited free volume of their molecular structure. Nevertheless, once there is a defect in the organic coating or once there is enough water inside the polymer matrix, there is a transport link that connects the aqueous phase with the coating and the metal oxide film, through which water and hydrated ions migrate. This is the starting point for the deterioration of the coating first, and then of the oxide film and progressively of the metallic structure overall. The water molecules move toward the metal surface and they change the polymer properties. At the metal surface, they may replace the polymer and interact with the metal oxide film by opening a path for charged species [7, 8]. After the interaction with the metal oxide, electrochemical processes may start. With the creation of corrosion products underneath the coating, osmosis may be induced, creating mechanical forces that tend to separate the polymeric layer from the metal substrate [9] and cause local deformations [10, 11].

The diffusion of water and ions into the coating can be described in first approximation using Fick's law of diffusion, which describes these phenomena for a steady state (Eq. (1)):

$$J = -D\frac{(\partial c)}{(\partial x)} \tag{1}$$

where J is the diffusion flux, D is the diffusion coefficient, c is the concentration and x is the direction of the diffusion. To predict the water accumulation rate at non-steady state, Fick's second law of diffusion can be used (Eq. (2)):

$$\frac{\partial c}{\partial t} = D\left(\frac{\partial^2 c}{\partial x^2}\right) \tag{2}$$

where t is the diffusion time. This equation considers the coating as a homogeneous layer, where the diffusion takes place in one dimension and the diffusion coefficient is independent of distance, concentration and time. The temperature dependence of the Fickian diffusion of water is supposed to follow an Arrhenius model, as long as the temperature is below the glass

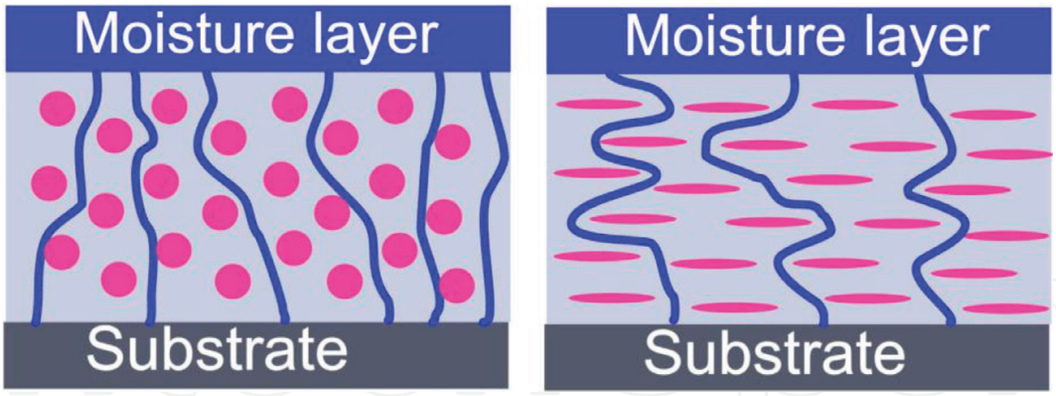

Figure 1. Spherical pigments allow easy penetration of water while lamellar pigments create more tortuous thus longer pathways for diffusion [23].

transition temperature (T_g) of the polymer. However, there are cases in which the transport of penetrants swells the polymer and changes the sorption kinetics, resulting in a non-Fickian diffusion process. This is common in more hydrophilic polymers, where the penetration of water plasticizes the polymer matrix. If this decreases the T_g (of the amorphous fraction) of the matrix sufficiently to have a change from a glassy to a rubbery state, diffusion may become 2–3 orders of magnitude faster. In addition, temperature variations during absorption, can permanently and significantly alter sorption behavior. The diffusion of water molecules in some organic coatings (e.g. epoxy) has been approached either volumetrically or interactionally [12]. The volumetric approach is based on the diffusion of water molecules through the free volume that present in between the macromolecular chains or the chain segments of the crosslinked network [13–16]. The free volume and the diffusion phenomenon depend on the crosslinking density and the physical state of the polymeric matrix. The nature of the penetrants (size, shape and polarity) influences the permeability and the rate of transport within the matrix. It has been reported that an increase in the size of the penetrant molecules causes a decrease in the diffusivity [17–19]. On the contrary, the interactional approach is based on the interactions between the polar groups and the water molecules, considering in general, the chemical nature of the components [20–22]. In general, the diffusion coefficient depends on the chemical functional groups and of the micro-organization of the polymer (void spaces, crosslinking and crystallinity). The presence of fillers and additives in the coating influences the chemical nature hence the diffusion coefficient too. **Figure 1** is an illustration of how the shape of the pigments in the coating may influence the pathway through which the water will manage to reach the substrate [23].

3. Experimental measurements of water sorption and transport

When a dry coating is exposed to an aqueous solution, water and ions slowly permeates the coating structure. There are many techniques to assess the transport properties of electrolyte in the coating film. In this section, we present the most common experimental methods to study the water uptake in organic coatings. There are two basic types of analysis: those which try to calculate the diffusion rates and those trying to demonstrate the concentration profiles. The

most classic techniques are the gravimetric method (GM), attenuated total reflection Fourier transform infrared spectroscopy (ATR-FTIR), nuclear magnetic resonance (NMR) and electrochemical impedance spectroscopy (EIS). At the end of this section, we introduce a novel, non-destructive technique for evaluation of water penetration in coatings: terahertz spectroscopy (time-domain (TDS) and frequency-domain (FDS)).

3.1. Gravimetric method (GM)

The gravimetric method is probably the oldest method to determine the sorption of water by a coating. It is still widely used because it is a simple and accurate way by measuring the total weight gain after exposing the coating to liquid or vapor for a period of time. Different (weighing) equipment is used depending on the sensitivity required. The sample, usually a coated metal substrate or a free-standing coating, is immersed in the electrolyte and removed for weighing at different points of time. It is essential to wipe the excess liquid from the exposed surface before placing the sample on a microbalance. The weight gain (Eq. (3)) at time t, assuming a constant penetration of liquid in an initially completely dry film of thickness L, is described by Crank and Park [24]:

$$\frac{M_t}{M_\infty} = 1 - \frac{8}{\pi^2}\sum_{n=0}^{\infty}\frac{1}{(2n+1)^2}\,exp\left[\frac{-D(2n+1)^2\pi^2 t}{L^2}\right] \tag{3}$$

where M_t is the absorbed mass at time t, M_∞ is the equilibrium mass and D is the diffusion coefficient that is assumed to be constant. This formula considers that the uptake of solute into polymers is following Fick's law. Kloppers et al. [25] investigated the water uptake in PET films of different thickness. **Figure 2** shows that the water diffusion is Fickian and that the relative mass change M_t/M_∞ versus the dimensionless time $\tau = tD/L^2$ plot, can be described by the Eq. (3).

3.2. Attenuated total reflection Fourier transform infrared spectroscopy (ATR-FTIR)

The diffusion of water in an organic coating can also be followed using attenuated total reflection Fourier transform infrared spectroscopy (ATR-FTIR) [26, 27]. Infrared spectroscopy provides quantitative information on the composition of complex molecules or mixtures of molecules, by studying the absorption of IR light resulting from vibrations of functional groups. As typically the thickness of a polymer film studied in transmission needs to be less than 10 μm to avoid complete absorption in sections of the spectral region, often ATR-FTIR is used for thin coatings. In ATR-FTIR, the IR beam passes through the ATR crystal (often germanium, silicon, ZnSe or diamond) and reflects at the interface between the crystal and the sample. This reflection creates an evanescent wave that penetrates into the coating to a depth of a few micrometers. The penetration depth depends mainly on the refractive indices of the ATR crystal and the material of the sample, the wavelength of the light beam, and the angle of incidence. The refractive index of the ATR crystal must be greater than the refractive index of the sample. The beam exits the crystal and it is collected by a detector, giving an ATR infrared spectrum. This technique allows for following the water sorption by an organic

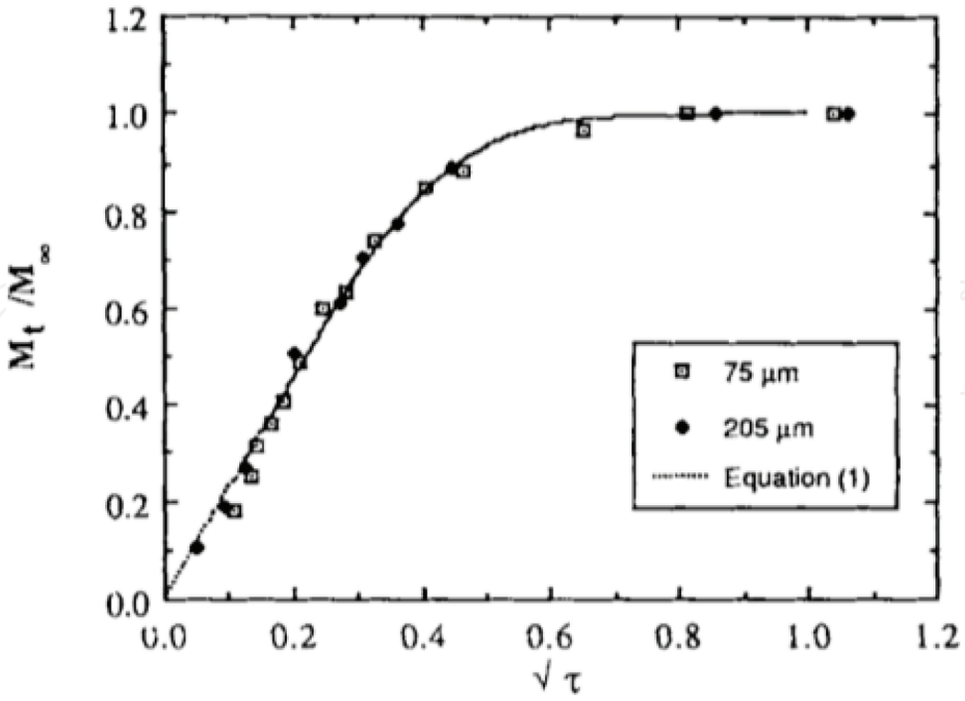

Figure 2. Water uptake against the square root of the dimensionless time, τ, for the PET films of 75 and 205 µm thickness and the theoretical result taken from Eq. (3) [25].

coating when it is exposed to an aqueous solution. Nguyen et al. [28] demonstrated a set-up that detects the water at the coating/substrate interface regardless the thickness of the coating and Fieldson and Barbari [26] and other researchers studied the water sorption kinetics in polymeric films [29]. Typically, the sample is a free-standing organic coating that is placed between the ATR crystal and the diffusing medium. With this method it is possible to measure the amount of absorbed water as a function of time, in experiments taking place in situ, by recording time-resolved IR spectra of the hydroxyl (νO–H stretch) absorption band, typically in the range of 3000–4000 cm^{-1}. It is essential that the coating is in direct contact with the crystal. Recently, several polymeric materials have been analyzed for water sorption and desorption in this way [30–34]. Wapner et al. [35, 36] used a similar experimental set-up as in **Figure 3**, to measure the uptake of water and ion transport at polymer/metal interface. They used deuterated water instead of normal water because the IR-Bands of the former do not overlap with the bands from the epoxy resin.

The principle behind the quantitative analysis of the spectra is the direct relationship between the absorption of electromagnetic waves and the quantity of the absorbing material. For transmission FTIR, the Beer–Lambert law represents this relationship (Eq. (4)):

$$dI = -\varepsilon \ln 10\, cI\, dz \tag{4}$$

where I is the light intensity at position z, ε is the molar absorption, c is the concentration of absorbing substance. By integrating Eq. (4), the concentration profile over the thickness of the film is accounted for (Eq. (5)):

$$A = -\log \frac{I}{I_0} = \int_0^L \varepsilon c \, dz \tag{5}$$

where A is the measured absorbance, I_0 is the intensity of the incident light, I is the intensity of the transmitted light, L is the thickness of the coating, over which there is the absorbing group.

In ATR-FTIR, the evanescent wave field decays exponentially in the less medium according to Eq. (6), and the penetration depth of the evanescent IR beam into the sample is the reciprocal of Eq. (7):

$$E = E_0 e^{-\gamma z} \tag{6}$$

$$\gamma = 2n_2\pi \frac{\sqrt{sin^2\varphi - \left(\frac{n_1}{n_2}\right)^2}}{\lambda} = \frac{1}{d_p} \tag{7}$$

where E_0 is the electrical field strength at the interface, I equals E^2, z is the distance from the surface, n_1 is the refractive index of ATR crystal and n_2 is the refractive index of the coating, φ is the angle of incidence of the infrared beam and d_p is the depth of penetration of the IR beam into the sample. Assuming Fickian diffusion, the diffusion coefficient can be calculated by the equation that describes the intensity at a given point as a function of the electrical field (Eq. (8)):

$$\frac{A_t}{A_\infty} = 1 - \frac{8\gamma}{\pi\left[1 - \exp\left(-2L\gamma\right)\right]} \left[\frac{\exp\left(-\frac{D\pi^2 t}{4L^2}\right)\left(\frac{\pi}{2L}\, exp\left(-2\gamma L\right) + \left(2\gamma\right)\right)}{\left(4\gamma^2 + \frac{\pi^2}{4L^2}\right)} \right] \tag{8}$$

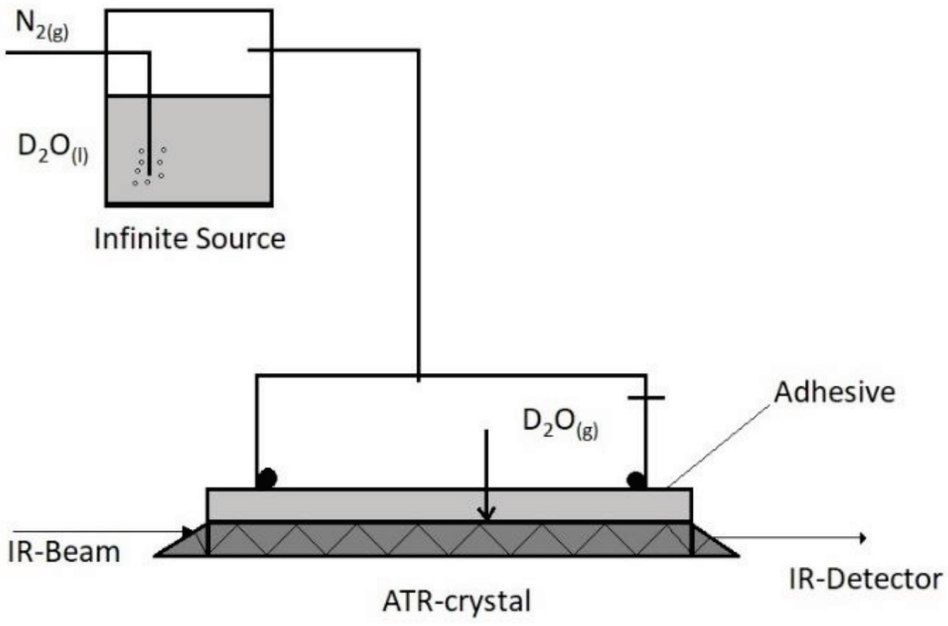

Figure 3. Experimental set-up for the measurement of water diffusion using ATR-FTIR. The deuterated water was used instead of water as the IR-Bands of the deuterated water do not overlap with bands from the epoxy resin [35].

where A_t is the absorbance at time t, A_∞ is the absorbance at equilibrium, and D is the diffusion coefficient [25]. In the IR spectrum, each stretching and bending vibration occurs with a characteristic frequency as the atoms and charges involved are different for different bonds. Typical difference ATR-FTIR spectra for the water absorption in an alcohol/amine adhesive film exposed to an atmosphere saturated with deuterated water (D_2O) for different exposure times has been demonstrated by Wapner et al. [35] in **Figure 4**. They also calculated the diffusion coefficient based on the increase of the area of the νOD-band and by fitting that curve with Eq. (8). The negative νO–H bands are because deuterated water molecules (D-protons) replaced the H-protons of the polymer and lowered the intensity of the νO–H absorption bands (the higher mass of the D atom shifts the wave number to lower values). According to Nguyen et al. [37], the idea behind the increasingly negative CH_x bands is that the water replaces the polymer at the interface and builds up an aqueous layer, leading to a gradual loss of adhesion. Given that penetration depth of the IR beam is nearly constant during an experiment, the lowering in the intensity of the polymer bands occurs as the polymer is pushed away by the developing aqueous layer.

The quantification of water at the coating/substrate interface is derived from the penetration depth concept of internal reflection spectroscopy developed for thin and thick films. Supposing that l is the thickness of the water layer at the coating/substrate interface; d_{pw} and d_{pc} are the penetration depths of the evanescent wave in water and coating, respectively; n_2 is the refractive index and α_2 is the absorption coefficient of water at the coating/substrate interface, then the thickness of the water is given by Eqs. (9) and (10):

$$l = \frac{d_{pw}}{2}\left[-\ln\frac{1-\frac{A}{A_\infty}}{1-c_w\frac{d_{pc}}{d_{pw}}}\right] \tag{9}$$

$$A_\infty = \frac{n_2\alpha_2 E_0^2 d_{pw}}{2n_1\cos\theta} \tag{10}$$

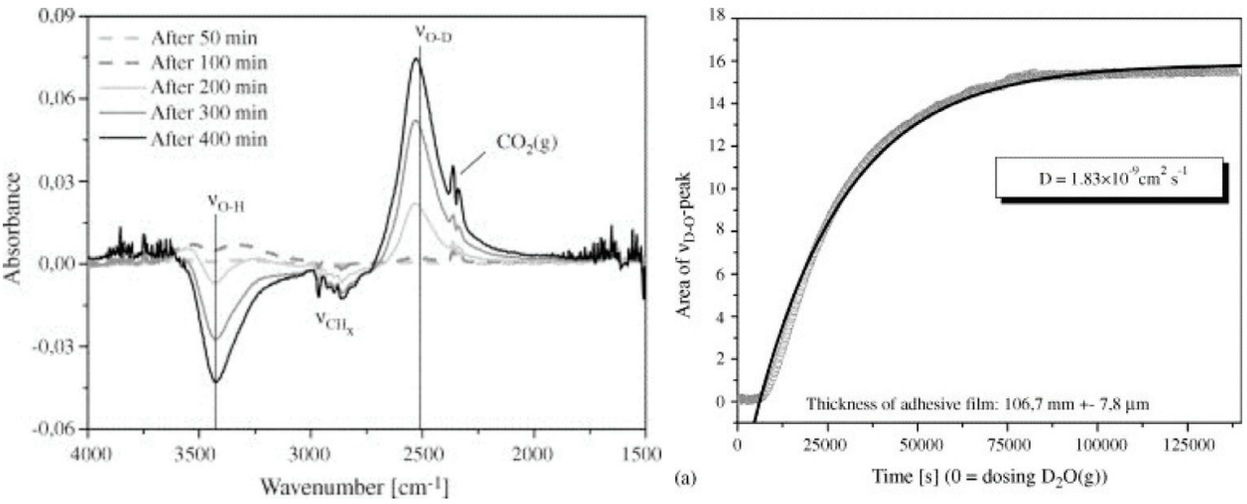

Figure 4. On the left plot, the difference IR spectra of deuterated water diffusion in an adhesive film on silicon ATR crystal by ATR-FTIR is shown, and on the right plot, measurement of the diffusion coefficient of deuterated water is shown [35].

where c_w is the fraction of water sorbed in the coating within the probing depth and A_∞ is the IR absorbance when the water layer at the coating/substrate interface is very thick. The amount of water Q is given by Eq. (11) where α is the area in contact with water and ρ is the density of water at the interface:

$$Q = l\alpha\rho \tag{11}$$

3.3. Nuclear magnetic resonance (NMR)

Nuclear magnetic resonance (NMR) is a spectroscopic technique based on the absorption of electromagnetic radiation in the radio frequency range (4–900 MHz). It is widely used to obtain structural information or even identify molecules in solution. Compared to IR spectroscopy, NMR can also provide information on molecular dynamics.

NMR takes advantage of the spin states of protons or other atoms with a non-zero spin. In a (static) magnetic field, the nuclei resonate at a specific resonance frequency between states with a magnetic moment parallel and opposite to the external field. Thus, the energy levels of the nucleus are split by the magnetic field, and nuclei can be excited from the lower to the higher level by a radio frequency (RF) pulse. More specifically, Eq. (12) shows the linear dependence between the resonance frequency and the magnitude of the applied magnetic field:

$$f = \frac{\gamma}{2\pi} |\vec{B}| \tag{12}$$

where f is the resonance frequency in MHz, γ is a constant and the ratio $\gamma/2\pi$ is the gyromagnetic ratio and it is different for different kinds of nuclei. $\left|\vec{B}\right|$ is the magnitude of the applied magnetic field in tesla (T) [38, 39]. For example, the hydrogen nucleus has a constant γ = 42.58 MHz/T. By exciting the nuclei with a radio frequency pulse at the resonance frequency, the nuclei in return start emitting signals recorded by a receiver coil. The most common way of extracting chemical information from NMR signals is the chemical shift: the applied magnetic field induces currents in the electron cloud surrounding the nucleus, creating an induced magnetic field of opposite sign, reducing the field sensed by the nucleus. This induced field has a magnitude between 10^{-4} and 10^{-6} times the size of the applied field.

NMR relaxometry can provide information about the diffusivity of liquids [40] and the mobility of the polymer molecules [41]. After giving an RF-pulse (e.g., a 90° or 180° pulse), the magnetization will relax to its equilibrium state through spin lattice and spin–spin relaxation, characterized by relaxation times T_1 and T_2, respectively, which are very sensitive to the molecular motion. For T_2 relaxation, a CPMG sequence is used, leading to a signal S described by the multiexponential decay given in Eq. (13):

$$S(t) = \sum_i S_i e^{-t/T_{2i}} \tag{13}$$

where the S_i is the component intensity, t is the time from the 90° pulse, and T_{2i} is the component relaxation time, which will increase with the mobility of the component. Thus, the

components of the signal decay are correlated with coating components and their mobility. For polymers, what matters is the segmental mobility of the polymeric chains. Hence, plasticizing effects of sorbed water can be detected since this phenomenon leads to a mobility increase of the polymer chains [42]. For water, the T_2 relaxation time will depend on the state (bound or free) and on the pore size distribution [43, 44].

Glover, Aptaker et al. [45, 46] proposed the GARField approach, a powerful magnetic resonance imaging (MRI) method that can be used for monitoring the ingress of water in coatings and the corresponding changes in molecular mobility [47]. Baukh et al. [38] used this approach to visualize the water distribution in multilayer polymeric films: using a high static gradient of the magnetic field generated by special shaped magnetic poles, depth profiles over 500 μm could be analyzed with a 2.5–6 μm resolution. The experimental set-up is shown in **Figure 5**.

For a multilayered film combining a top coat and a base coat on glass, the intensities of NMR profiles taken from both wet and dry coatings were compared. The signal intensity of the wet coating was higher than the intensity of the dry one (**Figure 6**). The polymer was also exposed to D_2O, which is expected to behave very similar to water molecules. Progressively, D_2O molecules affect the polymer matrix mobility, and as deuterium cannot be probed, the only detected NMR signal is from the polymer. This way it is possible to follow the mobility of the polymeric chains, reflected by the enhancement of the NMR signal.

The signal increase $\Delta S = [S_{D2O/H2O}\text{-}S_{D2O}]$, where S are the integrated signals of the base coat layer in the case of exposure to a D_2O/H_2O mixture and to pure water, respectively, is proportional to the mass of water in the coating Δm (mg) and can be written as $\Delta S = k\Delta m$, where k (mg^{-1}), is a proportionality coefficient given by (Eq. (14)):

$$k = \frac{1}{\rho_w A}\left[1 - exp\left(-\frac{t_r}{T_1}\right) exp\left(-\frac{t_e}{T_2}\right)\right] \tag{14}$$

where ρ_w is the density of liquid water, A is the area of the base coat, T_1 and T_2 are the relaxation times of water, and where t_r is the repetition time and t_e is the echo time of the pulse sequence used. Using this approach, the increase in water content in the base coat due to

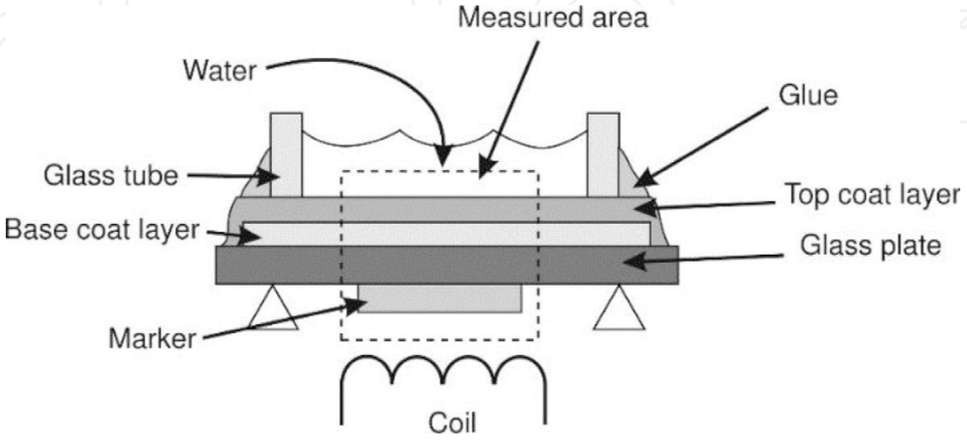

Figure 5. Schematic representation of the experimental set-up for the measurement of the water uptake using the GARField approach. The samples were put on top of the RF coil. To wet a sample, a glass tube was glued on top of the coating [38].

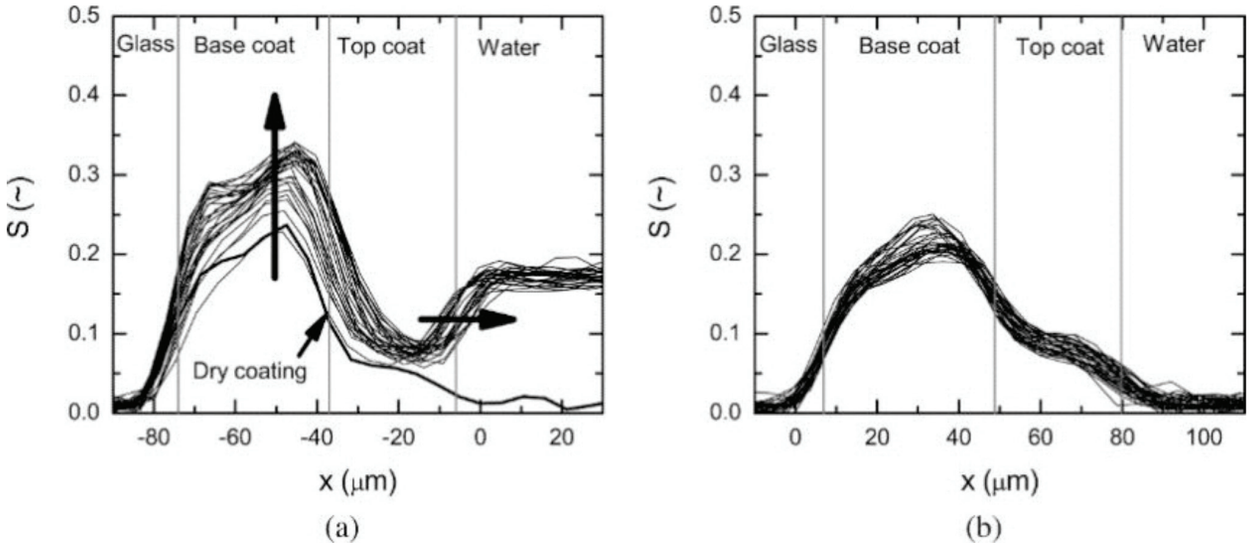

Figure 6. NMR signals profiles in the sample of base coat during (a) water and (b) heavy water uptake. The vertical arrow indicates the signal increase in the base coat and the horizontal arrow indicates swelling. The lower bold line in (a) represents the signal of the dry sample [38].

diffusion of water through the top coat can be followed, permitting an (indirect) estimation of the diffusion coefficient in the top coat.

If both diffusion and molecular mobility contribute to the relaxation process, the measured T_2 time will be given by (Eq. (15)):

$$\frac{1}{T_2} = \frac{1}{T_{2D}} + \frac{1}{T_{2S}} \tag{15}$$

where T_{2D} represents relaxation due to diffusion and T_{2S} relaxation corresponding to the mobility of the measured species. The relaxation due to diffusion in the field gradient is given by (Eq. (16))

$$T_{2D}{}^{-1} = \alpha\gamma^2 G^2 D t_e{}^2 \tag{16}$$

where D is the self-diffusion coefficient of the measured species, α is a constant defined by the evolution of coherent pathways for a given pulse sequence and is determined using the measurement of the diffusivity of pure water in a dilute aqueous reference solution, and G is the gradient of the magnetic field. Baukh et al. [48] estimated the self-diffusion coefficients of water in a fully and partially saturated base coat using the slope of the linear part of the $T_2{}^{-1}$ versus $t_e{}^2$ curve (Eq. (16)). For a more detailed explanation of the principles and equations, the reader is referred to the papers of Huinink and coworkers [38, 47, 48].

3.4. Terahertz spectroscopy: time-domain (TDS) and frequency-domain spectroscopy (FDS)

The frequency region of electromagnetic waves ranging from ~30 GHz to ~10 THz covers typically three bands, called as the mmw band, the sub-THz band and the THz-band which are situated between the microwave band and the infrared. In order to simplify the

terminology related to this spectral range, we call this spectral part range the THz domain, which is the least exploited of the electromagnetic spectrum. Nevertheless, recently spectroscopies methods operating in this region have been used for the characterization of various materials. THz radiation does not readily penetrate through metals or pure polar liquids such as water. However, this limitation of THz propagation through water turns into an advantage in detecting moisture or humidity in materials as water has a large relative permittivity and is highly absorptive in the THz range and at the same time the considered organic materials which absorb moisture are reasonably transparent for the lower frequencies of the considered THz band. Hence, the contrast in the image between the wet and the dry regions is high. Normally, the water diffusion in organic coatings takes some hours or days. In general, THz imaging systems can operate in the frequency or the time domain, the latter one featuring broadband characteristics, allowing low spectral resolution spectroscopy and typically more expensive, the former one allowing much higher spectral resolution. THz imaging systems can scan the full coating area in a few to tens of seconds, therefore allowing to follow the water ingress in the coating from the very early stages of the diffusion. Another property of THz imaging is the fact that it can produce 2D images of the water ingress and detect structures comparable in size to the electromagnetic wavelength of the THz radiation (from 10 mm down to 0.3 mm). For example, it can spot water diffusion into comparably-sized voids in the subjected material as it will create a large contrast between the dry and the wet THz absorbance images [49]. The first demonstration of THz imaging for mapping the moisture has been done in drying leaves [50, 51]. Overall, this method enables the creation of images of liquid diffusion in materials and depicts possible diffusion pathways, the extraction of average diffusion coefficients, and the non-destructive assessment of hydration levels inside objects. The high permittivity of water is mainly the feature that influences the contrast mechanism for moisture detection by THz imaging. The ingress of water in the material is followed by an increase of the overall absorbance at all THz frequencies.

Jordens et al. [52] studied the water absorption in polyamide and wood plastic composite using THz spectroscopy. By comparison with gravimetry results, they concluded that the refractive index and the absorption coefficient obtained (at 600 GHz) can be employed to derive the volumetric water content of a polymer from the measured THz signal after calibration. Although the contrast in permittivity between the coating material and the water is high, for very thin layers (sub-100 μm) with very low water content (only a few %), sensitivity enhancement techniques (e.g. resonant like structures) are needed [53, 54]. These techniques can only be implemented in the frequency domain. Recently, Pandey et al. [55] showed that mm-waves (around 60 GHz) can be used to follow the drying or freezing of food slices with high sensitivity. However, all the mentioned methods are not completely blind and need priori information (e.g. the thickness of the coating) to extract the absolute water content. Using dedicated setups exploiting the transient radar method, also the blind analysis of multilayer structures with deep submillimeter depth resolution, significantly below the wavelength, is feasible [56]. This method allows to determine the dynamic thickness of the coating (e.g. due to swelling) and the frontline of the water ingress.

Obradovic et al. [57] studied the diffusion coefficient of acetone in polycarbonate and polyvinylchloride polymers by using a THz reflective geometry (**Figure 7**). **Figure 8**, on the left shows THz time domain measurements presented as a stack plot as a function of

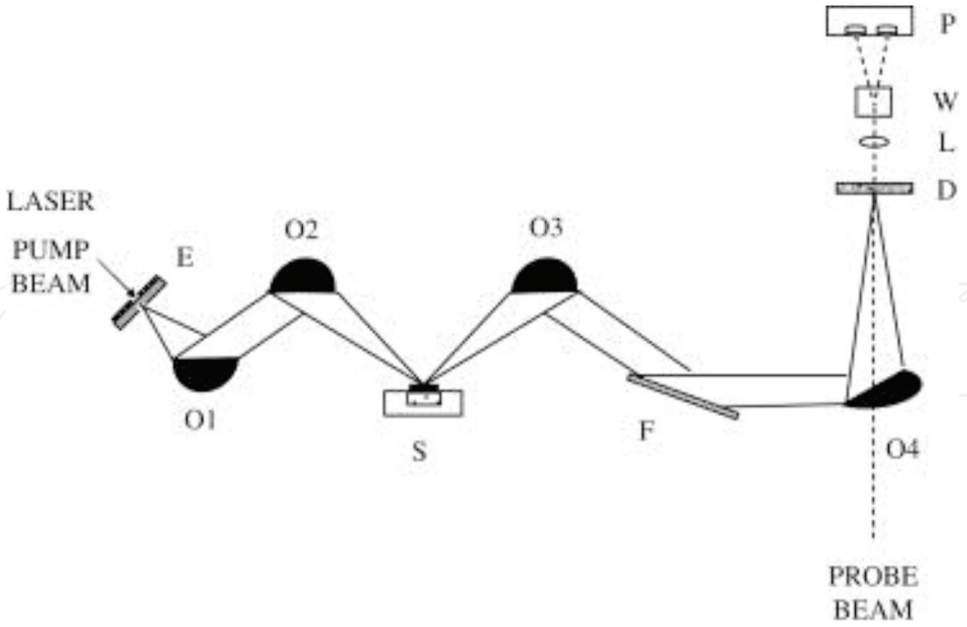

Figure 7. An illustration of the reflectance spectrometer. *E* is the emitter, *O* is the off-axis parabolic mirrors, *F* is the flat mirror, *S* is the sample holder with polymer disc, *D* is the detector, *L* is the lens, *W* is the Wollaston prism, and *P* is the photodiodes [57].

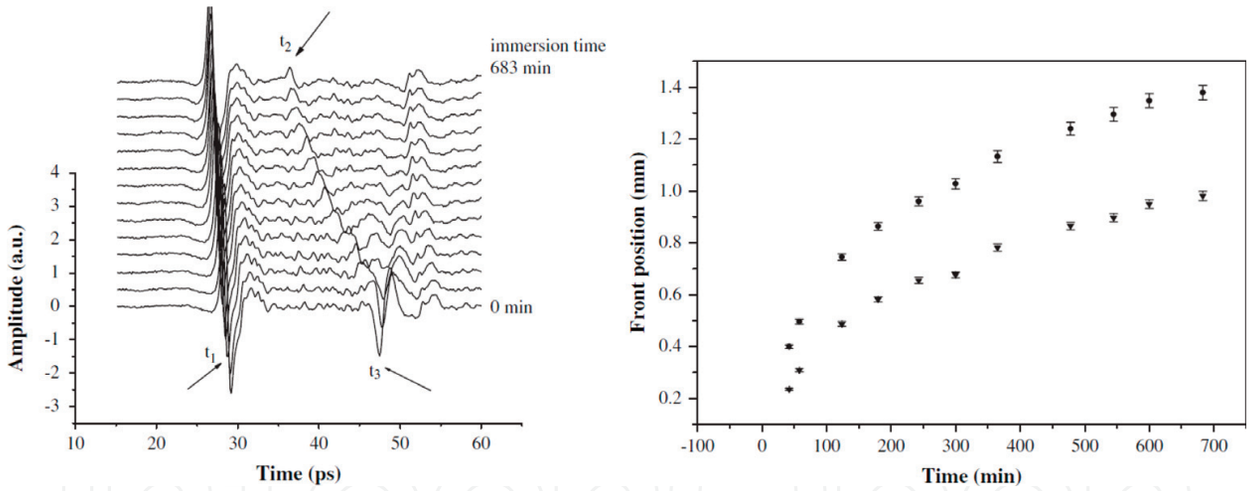

Figure 8. THz-time domain measurements of acetone ingress into PVC at room temperature. On the left the plot, the waveforms at time t_1 correspond to the top surface, at t_2, they come from the penetrant front interface and at time t_3, from the rear surface of the polymer. On the right plot, the acetone depth penetration into the polymer as a function to time is shown [57].

exposure time of the PVC to the acetone, and on the right, it shows the evolution of the depth of penetration of acetone versus time.

Although diffusion coefficients or quantitative diffusion models have not been determined yet using THz-TDS, the high sensitivity for water and the ability to measure with submillimeter depth resolution are promising for following concentration profiles during the ingress of water in coatings. Kusano et al. [58] studied the penetration of acid solutions into epoxy resins by THz-TDS. They found that the refractive index of epoxy specimens is changing as this is due to the solution uptake.

3.5. Electrochemical impedance spectroscopy (EIS)

Electrochemical impedance spectroscopy is an in situ, non-destructive technique that can be used to characterize a wide variety of electrochemical systems, including the degradation of the corrosion protection of coated metals over time. The EIS experiments are usually done in an electrochemical cell with three electrodes immersed in a liquid electrolyte: the working electrode, which is the coated metal, the counter electrode (made of an inert conductor, such as platinum) that provides a circuit along with the working electrode, and the reference electrode that is used to determine the potential of the working electrode (e.g. made of Ag/AgCl). The impedance is measured between the reference electrode and the working electrode. The electrochemical cell is connected to a potentiostat instrument that controls the voltage difference between the reference and the working electrode. Deflorian et al. [59] studied the ion diffusion through organic coatings with EIS, working in the electrochemical cell of **Figure 9**.

In general, EIS involves measuring the electrical response of a system subdued to a low amplitude, sinusoidal potential perturbation (Eq. (17)), typically in the range of ±10 mV, as a function of frequency, usually between 10^{-2} and 10^{5} Hz. The response of the system is an alternating current signal with the same frequencies (the linear part of the response, Eq. (18)) and higher harmonics (the non-linear part):

$$E(t) = E_0 \cos(\omega t) \tag{17}$$

$$I(t) = I_0 \cos(\omega t - \varphi) \tag{18}$$

where E_0 is the amplitude of the potential difference, I_0 is the amplitude of the current, $\omega = 2\pi f$ is the angular frequency and t is the time, φ is the phase shift, time shift or phase angle, and it exists because the response depends on the physicochemical processes taking place. In

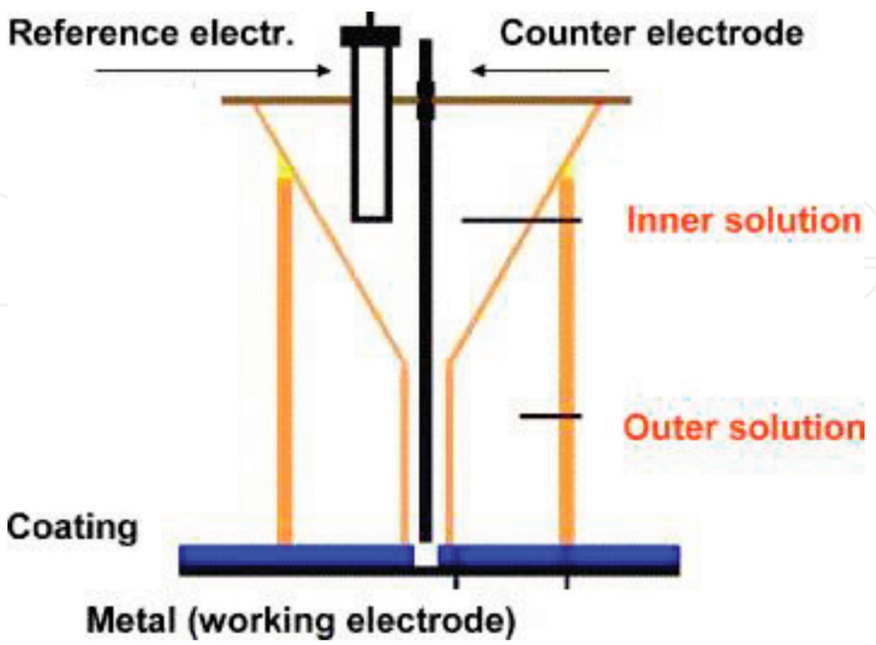

Figure 9. Electrochemical cell with three electrodes (working, counter and reference) for analyzing the diffusion of water into a coating [59].

corrosion studies, the current response is not linear due to polarization and/or passivation effects. However, for small perturbation signals, the response may behave as pseudo-linear.

Electrochemical processes that may take place in the coating-oxide-metal system can be described by equivalent electrical circuits consisting of a series of resistors, capacitors, and inductors, sometimes extended with special elements, like a Warburg element (when the system is dominated by mass transport phenomena). More specifically, the recorded impedance spectra are analyzed by fitting electrochemical equivalent circuits to the data. The change of certain parameters in the circuits can then be correlated with specific changes in the system over time, such as, an increasing permittivity of the coating that results from an increasing water sorption. The most simple electrical circuit would be a circuit with an electrical resistance only, defined by Ohm's law and mathematically expressed in Eq. (19):

$$R = \frac{E}{I} \tag{19}$$

where R is the resistance, E is the applied alternating potential difference, I is the alternating current response. For complex systems, the equivalent circuits get more complicated, and one needs to move from the real to the imaginary representation, introducing the concept of impedance (Z). By turning Eqs. (17) and (18) into complex functions, the potential (Eq. (20)) and the current (Eq. (21)) are described as follows:

$$\widetilde{\boldsymbol{E}}(\boldsymbol{t}) = \boldsymbol{E_0}\, \boldsymbol{exp}\left(\boldsymbol{j\omega t}\right) \tag{20}$$

$$\widetilde{\boldsymbol{I}}(\boldsymbol{t}) = \boldsymbol{I_0}\, \boldsymbol{exp}\left(\boldsymbol{j\omega t} - \boldsymbol{\varphi}\right) \tag{21}$$

where j is the complex number ($j^2 = -1$). The measured potential and current are the real parts of the imaginary functions. The impedance is a measure of an electrical circuit's opposition to an alternating current when an alternating potential is applied. In analogy with Ohm's law, the impedance Z is expressed as (Eq. (22)):

$$Z = \frac{\widetilde{E}(t)}{\widetilde{I}(t)} = Z_0\, exp\,(j\varphi) = Z_0(\cos\varphi + j\sin\varphi) \tag{22}$$

where the impedance Z is a complex function with magnitude or modulus Z_0 expressed in ohms. The impedance consists of a frequency dependent real and imaginary part, which can be plotted in a Nyquist plot (**Figure 10**). Alternatively, the magnitude Z_0 and the phase angle φ of the impedance can be plotted as a function of frequency, giving the Bode plot (**Figure 12**). The semicircle of **Figure 10** reflects the impedance of a Randle's circuit and is characteristic for a single time constant. For more complex circuits, the Nyquist plot may contain several semicircles and often only a portion of a semicircle can be seen.

One of the important electrical elements for modeling the electrolyte-coating-oxide-metal system is the capacitor. The classical capacitor is composed of a non-conductive medium (dielectric) between two conductive plates. The capacitance depends on the dielectric properties of the medium, on the thickness of the medium, and on the size of the plates. For coating evaluation, taking a coated metal immersed in an electrolyte, the water represents one plate

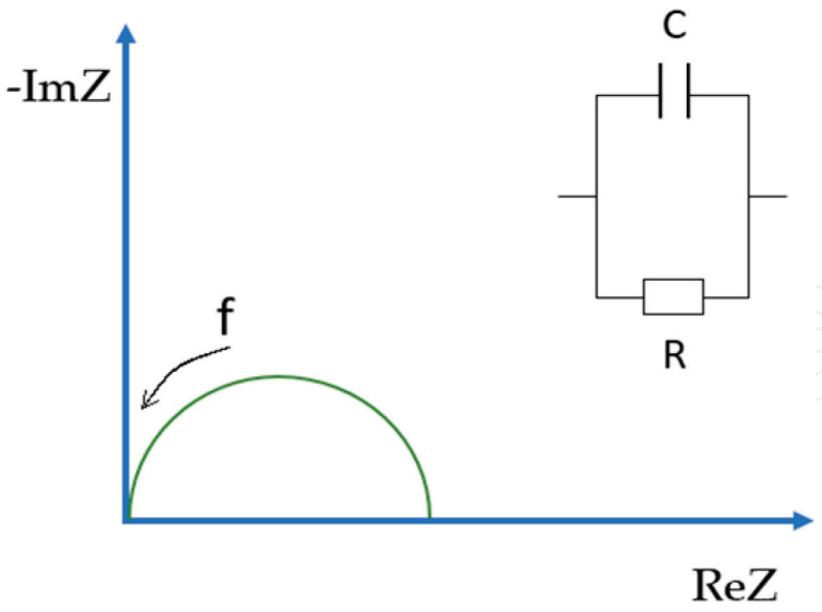

Figure 10. Nyquist plot for Randle's circuit made of a resistor in parallel with a capacitor.

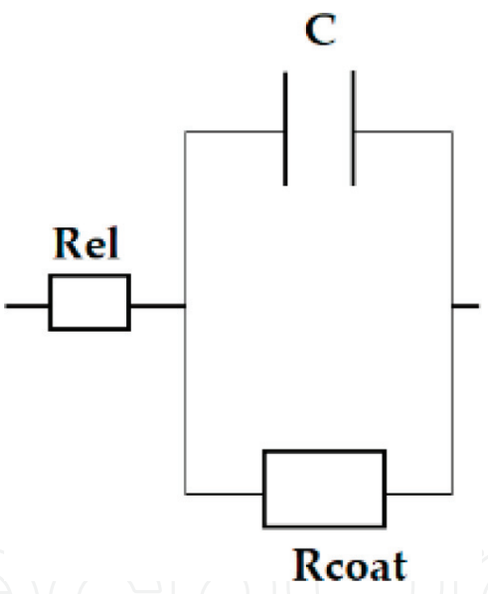

Figure 11. Equivalent circuit of coated metal system immersed in an electrolyte solution.

and the metal represents the other one, while the coating between the electrolyte and the metal can be considered as the non-conductive medium (the dielectric). Thus, EIS can be used to measure in situ the capacitance of the coating on metal system during exposure. The simplest equivalent electrical model that represents a coated metal immersed in an electrolyte is given by **Figure 11**, where R_{el} is the resistance of the electrolyte, C is the capacitance of the coating, and R_{coat} is the resistance of the coating.

The relation between the capacitance and the permittivity of the polymer is given by Eq. (23):

$$C = \frac{\varepsilon_r \varepsilon_o A}{d} \tag{23}$$

where C is the capacitance derived from the impedance measurements (expressed in F), ε_r is the relative permittivity of the coating (dielectric constant), ε_o is the permittivity in vacuum (in F), A is the surface of the coated metal, and d is the thickness of the coating. Typically, the dielectric constant of organic coatings is between 2 and 7, whereas the dielectric constant of water is 80.1 at 20°C. The diffusion of water into a coating increases the polarisability, and hence the permittivity of the polymer. Therefore, the absorption of water by the coating causes an increase in the capacitance, making EIS suitable to follow the absorption of water in a coating [60]. The magnitude of the impedance measured, represented by the electrochemical circuit of **Figure 11**, tends to decrease and the phase angle starts to increase as the coating absorbs water. The coating is considered bad when the coating impedance at low frequencies drops below 10^7 Ωcm^2 (this is evaluated per cm^2 of coating exposed to the electrolyte). Fredj et al. [61] studied the water ingress in epoxy organic coatings by EIS. **Figure 12** shows the Bode plots of an epoxy coating immersed in an electrolyte for different times of immersion, showing the impedance magnitude and (minus) the phase angle as a function of frequency. The phase angle starts from -90°, reflecting the (predominantly) capacitive behavior of the initial coating. For long immersion times, the phase angle at low frequencies evolves to zero, indicating a (predominantly) resistive behavior at these frequencies.

According to Deflorian et al. [62] the ideal coating capacitance increases in three phases, as indicated in **Figure 13**. Phase I represents a situation where the electrolyte diffuses homogeneously into the coating and usually it is described mathematically by Fick's first law (Eq. (1)). In phase II, the plateau represents the water saturation in the polymer matrix, where the capacitance remains constant over time. Finally, phase III shows a further increase of the water inside the coating, most probably in a non-homogeneous way, due to (local) chemical changes in the coating.

The capacitance values derived using equivalent electrical models can be exploited to quantify the water volume fraction through the Brasher/Kingsbury [63, 64] equation (Eq. (24)):

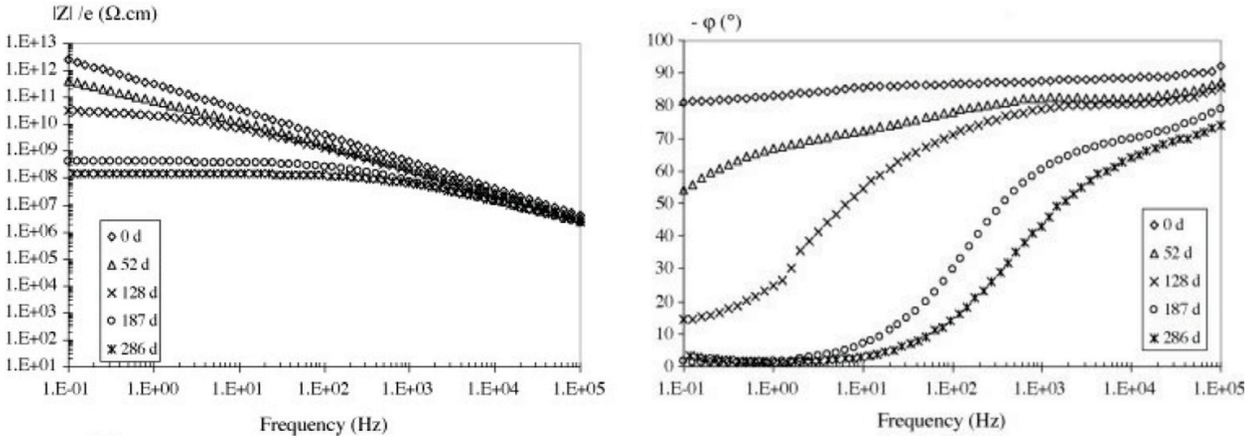

Figure 12. Bode plots for an epoxy coating immersed in sodium chloride solution for increasing times [61]. Note that the impedance shown here in ohm.cm, is the impedance measured per cm^2 coating surface and per cm coating thickness, which is suitable for evaluating the coating material.

$$V_t = 100 \frac{\log \frac{C_m}{C_{m,o}}}{\log \varepsilon_w} \tag{24}$$

where V_t is the water volume % of water absorbed, C_m is the measured capacitance at time t, $C_{m,o}$ is the measured capacitance at time zero, and ε_w is the dielectric constant of water at the experiment temperature T. The use of Eq. (24) considers some of the following assumptions: the change in capacitance of the coating is only due to an increase in absorbed water, the water is well distributed throughout the coating, no swelling occurs due to the gradual water uptake, no interactions occur between water and polymer molecules. If these assumptions are not fulfilled, then there is a possibility of overestimating or underestimating the water content. By estimating the water content from the capacitance, it is also feasible to calculate the kinetics of water uptake (diffusion coefficient) [65, 66]. Starting from Fick's second law and the use of the value of the capacitance at different immersion times, the following formula is used (Eq. (25)) [67]:

$$\frac{C_m - C_o}{C_\infty - C_{m,o}} = \frac{4\sqrt{D}}{d\sqrt{\pi}} \sqrt{t} \tag{25}$$

where D is the diffusion coefficient, and C_∞ is the capacitance at saturation. In this approach, it is assumed that the water ingress follows a Fickian relation, although, as mentioned above, this is not always the case.

Working on coating films with EIS and the gravimetric method, and using a more complex equivalent circuit that includes constant phase elements (CPE), Nguyen et al. [68] suggested that in some cases the first step of the diffusion process can be described by Fick's law, but during the second step (water saturation state) the diffusion process is described by non-Fickian behavior due to swelling (**Figure 14**).

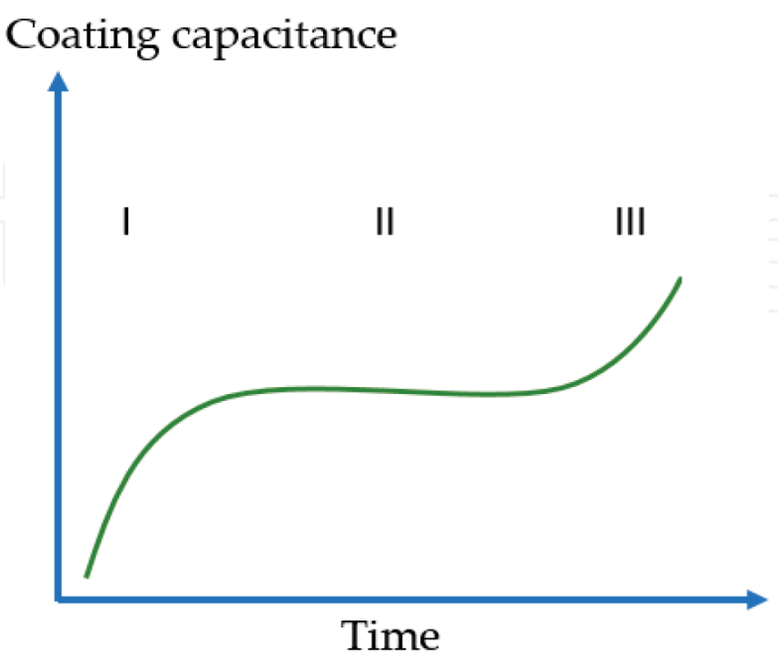

Figure 13. Coating capacitance evolution as a function of time for coatings exposed to an aqueous solution (*redrawn after* [62]).

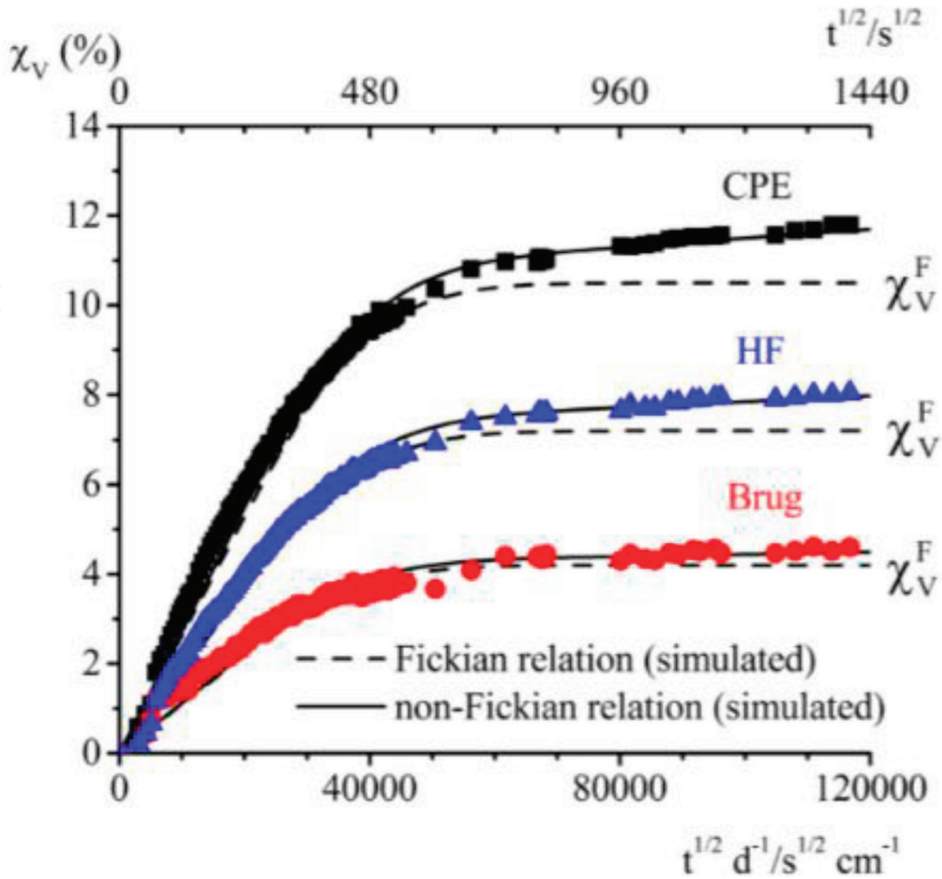

Figure 14. Evolution of the volumetric water content χ_v for unstressed coating films in a 3 wt.% NaCl solution, immersed at 30°C, calculated using the film capacitance at high frequencies C_{HF}, the film capacitance equivalent CPE, and the "true" film capacitance C_{Brug} [68].

4. Discussion

In the previous section, the most common techniques to measure or follow the water uptake in organic coatings were introduced, complemented with the time-resolved or spectrally resolved THz-method that was recently developed. **Table 1** shows the experimental characteristics and the limitations and **Table 2** shows the advantages and disadvantages of each technique.

In most diffusion studies, researchers work on two or more techniques to obtain complementary information. No matter the number of studies done so far to extract the diffusion coefficients of the electrolyte, the detailed analysis of moisture diffusion in polymer film and coatings—including the dependence on moisture content, temperature, salt concentration, pigments,…—has never been comprehensively determined. In fact, the determination of such relationships requires the measuring of time-dependent penetrant concentration profiles in thin polymer film or coatings. This is hard to achieve, not only because of the heterogeneous nature of most coatings, but also because of the insufficient penetration depth (ATR-FTIR) or depth resolution (NMR, terahertz spectroscopy), or because of the inability of the measuring techniques to study the concentration gradient directly (GM, EIS). THz spectroscopy (THz-TDS and THz-FDS), EIS, and GM can be applied to coatings of thicknesses of several millimeters. For thick coatings, the high impedance limits the suitability of commercial instrumentation.

	GM	ATR-FTIR	NMR	THz: TDS and FDS	EIS
In situ/ex situ	Ex situ	In situ and ex situ	In situ and ex situ	In situ and ex situ	In situ
Penetration depth d_p	$d_p \geq \mu m$	$nm \leq d_p \leq 5\ \mu m$	$d_p \geq \mu m$	$\mu m \leq d_p \leq cm$	$\mu m \leq d_p \leq mm$
Measurements	Weight difference between wet/dry conditions	Peak intensities corresponding to OH absorptions	Change in signal intensity depth profiles between wet and dry coatings	Imaging: contrast between wet and dry regions Coatings: change in reflection coefficient	Coating capacitance derived from impedance spectra using electrical equivalent models

Table 1. Experimental characteristics of all techniques.

The more complex the coating is, the more difficult it is to obtain valid diffusion coefficients. Methodological difficulties of separating the contributions of adsorption, absorption, capillary condensation…, make it difficult to establish a single model for obtaining accurate quantitative evaluations of an organic coating. In general, these effects are studied qualitatively rather than quantitatively. Additives, pigments and fillers further affect the equilibrium parameters (solubility or equilibrium water volume fraction) and the diffusion kinetic parameters (diffusion coefficient and permeability). For example, the presence of additives in the polymer can significantly increase solubility and equilibrium sorption values of water in the coating, thereby increasing the permeability. Of the techniques considered, EIS is most sensitive to (macroscopic) heterogeneity and defects in the coating (pinholes, particle aggregates,…).

For some of the techniques (ATR-FTIR, NMR) the use of free-standing films can be advantageous, however, this may affect the water migration. Holtzman [70] showed that transport of water in coatings applied on substrates is slightly lower than in free films. However, Rosen and Martin [71] found that in epoxy coatings applied to steel substrates, the diffusion coefficient is three times greater than those in free films. Internal stresses residing in the polymer after production probably play an important role. So, care must be taken in directly comparing results of layers prepared in different ways (free-standing or not, substrates, curing or drying protocol,…).

GM is a standard technique that allows fast measurements of the weight difference between the dry and the wet sample. The main drawback of this method is its sensitivity to the sample handling: a small excess of liquid on the surface or evaporation losses of volatile components may have a big impact on the results. Therefore, this method is not suitable for studying the initial stages of diffusion. However, it is often used as a complementary technique.

EIS is a powerful technique as it gives information on the very early stages of the water uptake process, in addition to information on other processes, such as the subsequent corrosion process. However, the data are interpreted based on equivalent electric circuits. Hence, the validity of the result depends on the validity of the chosen model.

NMR relaxometry using the GARField approach and THz-TDS and THz-FDS look quite powerful but are not generally accessible yet.

	GM
Pros	• Direct and fast measurement • Simple experimental set-up • Low cost equipment • Often used as complementary technique
Cons	• Discontinuous measurements • Risk of low precision due to fast evaporation before measurement • Risk of low precision due to water surface layers of variable thickness • For small amounts of water absorbed in coatings on metal substrates: very small relative mass changes
	ATR-FTIR
Pros	• Simple experimental set-up • Information on interaction between water and polymer molecules • Can probe distribution of water parallel to the coating/substrate interface • On free-standing films, it is feasible to follow in situ and continuously the migration of water • Good reproducibility
Cons	• Small penetration depth • On coatings: discontinuous measurements • Contact between sample and ATR crystal is crucial and may change as coating absorbs water
	NMR relaxometry (GARField)
Pros	• Gradients in moisture content in 100-μm coatings on glass substrates can be measured with 3–6 μm depth resolution • Probe distribution of water in multilayered coatings with multiphase polymer layers • Distinction between free and bound water, interaction between water and polymer molecules
Cons	• Metal substrates interfere with NMR, but taking this into account might be feasible [68] • Probe not yet commercially available
	THz: TDS & FDS
Pros	• Very fast measurement • Feasible on coated metal • High penetration depth up to a few cm for the lowest frequencies of the sub-THz spectrum • In thicker coatings (>100 μm), measuring gradients might be feasible • Imaging mode: water diffusion into comparably-sized cracks, voids • Advanced frequency domain techniques allow very high resolution in the water content measurements, down to 0.0005% • Transient radar methodology allows simultaneous measurements of (swelling) thickness of the coating and its water content via a dielectric mixing model
Cons	• Application on water diffusion in coatings was introduced recently (limited set of results exists) • Basic instrument yet commercially available • More advanced sensor systems need to be custom designed
	EIS
Pros	• Fast measurements at high frequencies • Normally on coated metal, but feasible on free-standing films • Complete view of coating deterioration process. Distinction of all phenomena that occur in the system (water ingress, double layer creation at the interface, beginning of corrosion) • Measuring the decrease of the coating resistance gives qualitative and quantitative information about the coating performance
Cons	• Slow measurements at low frequencies • If the potential perturbation is too high, it may affect the coated/metal system (non-linear behavior) • Interpretation of measurement data based on equivalent electrical circuits • Results are sensitive to pin holes and coating defects in general • Surface treatment of metal substrate before coating application may affect the measurements

Table 2. Pros and cons of all techniques for measuring diffusion of water in coatings.

5. Conclusion

Organic coatings are widely used for corrosion protection of metallic structures and the detailed characterization of water ingress in coatings is therefore crucial. The complexity of organic coatings (chemical composition, crosslinking), the presence of a wide range of additives for ensuring a wide range of properties, in combination with the nature of the metal substrate and its surface treatments, makes the research of water uptake in coatings quite challenging. Each of the techniques presented above has advantages and limitations, so selecting the most appropriate one strongly depends on the purposes of the research and the coating characteristics. Knowing the diffusion coefficient and how it is affected by the different factors (composition, temperature, filler, aging…) is crucial for making reliable life time predictions of coatings based on limited sets of experimental results. Often, to illustrate the capability of a technique, model coatings are chosen in accordance with the limitations of that technique. Of course, to measure the diffusion behavior, the coatings must fulfill some criteria, such as chemical stability, homogeneous composition, well-dispersed fillers, defect free,…, otherwise the results will never be reliable. The basic characteristics and limitations of each technique are pointed out in **Table 1**, while the main advantages and disadvantages are discussed in **Table 2**. Given these points, it is clear that a combination of two or more techniques will usually be needed to provide a clearer overview of the water diffusion process in organic coatings.

Conflict of interest

The authors whose names are listed immediately above certify that they have no affiliations with or involvement in any organization or entity with any financial interest, or non-financial interest in the subject matter or materials discussed in this manuscript.

Author details

Zoi Manoli[1]*, Darja Pecko[1], Guy Van Assche[2], Johan Stiens[3], Ali Pourkazemi[3] and Herman Terryn[1]

*Address all correspondence to: zoi.manoli@vub.be

1 Research Group of Electrochemical and Surface Engineering (SURF), Vrije Universiteit Brussel (VUB), Brussels, Belgium

2 Physical Chemistry and Polymer Science (FYSC), Vrije Universiteit Brussel (VUB), Brussels, Belgium

3 Department of Electronics and Informatics (ETRO), Vrije Universiteit Brussel (VUB), Brussels, Belgium

References

[1] Funke W. Toward a unified view of the mechanism responsible for paint defects by metallic corrosion. Industrial & Engineering Chemistry Product Research and Development. 1985;**24**:343-347. DOI: 10.1021/i300019a001

[2] Stratmann M, Fese R, Leng A. Corrosion protection by organic films. Electrochimica Acta. 1994;**39**:1207-1214. DOI: 10.1016/0013-4686(94)E0038-2

[3] García SJ, Fischer HR, van der Zwaag S. A critical appraisal of the potential of self healing polymeric coatings. Progress in Organic Coating. 2011;**72**:211-221

[4] Bergman SD, Wudl F. Mendable polymers. Journal of Materials Chemistry. 2008;**18**:41-62. DOI: 10.1016/j.porgcoat.2011.06.016

[5] Szauer T. Electrical and electrochemical resistances for the evaluation of protective non-metallic coatings. Progress in Organic Coating. 1982;**10**:157-170. DOI: 10.1016/0300-9440(82)80014-3

[6] Inone PC, Garcia CM, Ruvolo-Filho A. Evaluating barrier properties of organic coatings by water permeation and electrochemical methods. Journal of Coatings Technology. 2003;**75**:29-36. DOI: 10.1007/BF02697918

[7] Henderson MA. The interaction of water with solid surfaces fundamental aspects revisited. Surface Science Reports. 2002;**46**:1-308. DOI: 10.1016/S0167-5729(01)00020-6

[8] Posner R, Ozcan O, Grundmeier G. Water and ions at polymer/metal interfaces. Posner. In: da Silva LFM, Sato C, editors. Design of Adhesive Joints under Humid Conditions. Vol. 25. Berlin: Springer; 2013. pp. 21-52. DOI: 10.1007/978-3-642-37614-6_2

[9] van Ooij WJ, Sabata A, Loison D, Jossic T, Charbonnier JC, Adhes J. Paint delamination from electrocoated automotive steels during atmospheric corrosion. Part I. Hot-dip galvanized and electrogalvanized steel. Science and Technology. 1989;**3**:1-27. DOI: 10.1163/156856189X00010

[10] Ogle K, Morel S, Meddahi N. An electrochemical study of the delamination of polymer coatings on galvanized steel. Corrosion Science. 2005;**47**:2034-2052. DOI: 10.016/j.corsci.2004.08.017

[11] Leng A, Streckel H, Stratmann M. The delamination of polymeric coatings from steel. Part 1: Calibration of the Kelvinprobe and basic delamination mechanism. Corrosion Science. 1999;**41**:574-557. DOI: 10.1016/S0010-938X(98)00166-8

[12] Bellenger V, Verdu J, Morel E. Structure-properties relationships for densely cross-linked epoxide-amine systems based on epoxide or amine mixtures. Journal of Materials Science. 1989;**24**:63-68. DOI: 10.1007/BF00660933

[13] Apicella A, Nicolais L, de Cataldis C. Characterization of the morphological fine structure of commercial thermosetting resins through hygrothermal experiments. In: Kaush HH, Zachman HG, editors. Characterization of Polymers in the Solid State I: Part A: NMR and

Other Spectroscopic Methods Part B: Mechanical Methods. Vol. 66. Berlin, Heidelberg: Springer; 1985. pp. 189-207. DOI: 10.1007/3-540-13779-3_21

[14] Adamson MJ. Thermal expansion and swelling of cured epoxy resin used in graphite/epoxy composite materials. Journal of Applied Physics. 1980;**15**:1736-1745. DOI: DOI 10.1007/BF00550593

[15] Apicella A, Tessieri R, De Cataldis C. Sorption modes of water in glassy epoxies. Journal of Membrane Science. 1984;**18**:211-225. DOI: 10.1016/S0376-7388(00)85035-8

[16] Johncock P, Tudgey GF. Some effects of structure, composition and cure on the water absorption and glass transition temperature of amine-cured epoxies. British Polymer Journa. 1986;**18**:292-302. DOI: 10.1002/pi.4980180504

[17] Fujita H, Kishimoto A, Matsumoto K. Concentration and temperature dependence of diffusion coefficients for systems polymethyl acrylate and n-alkyl acetates. Transactions of the Faraday Society. 1960;**56**:424-437. DOI: 10.1039/TF9605600424

[18] Prager S, Bagley E, Long FA. Diffusion of hydrocarbon vapors into polyiso-butylene. II. Journal of the American Chemical Society. 1953;**75**:1255-1256. DOI: 10.1021/ja01101a517

[19] Soney CG, Sabu T. Transport phenomena through polymeric systems. Progress in Polymer Science. 2001;**26**:985-1017. DOI: 10.1016/S0079-6700(00)00036-8

[20] Zhou J, Lucas JP. Hygrothermal effects of epoxy resin. Part I: The nature of water in epoxy. Polymer. 1999;**40**:5505-5512. DOI: 10.1016/S0032-3861(98)00790-3

[21] Zhou J, Lucas JP. Hygrothermal effects of epoxy resin. Part II: Variations of glass transition temperature. Polymer. 1999;**40**:5513-5522. DOI: 10.1016/S0032-3861(98)00791-5

[22] Bouvet G, Dang N, Cohendoz S, Feaugas X, Mallarino S, Touzain S. Impact of polar groups concentration and free volume on water sorption in model epoxy free films and coatings. Progress in Organic Coating. 2016;**96**:32-41. DOI: 10.1016/j.porgcoat.2015.12.011

[23] Lyon S, Bingham R, Mills DJ. Advances in corrosion protection by organic coatings: What we know and what we'd like to know. Progress in Organic Coating. 2017;**102**(Part A):2-7. DOI: 10.1016/j.porgcoat.2016.04.030

[24] Crank J, Park GS. Methods of measurement. In: Crank J, Park GS, editors. Diffusion in Polymers. London, UK: Academic Press, Inc.; 1968. pp. 1-39

[25] Kloppers MJ, Bellucci F, Latanision RM, Brennan JE. Transport of dielectric properties of poly(ethylene terephthalate) as determined via electrochemical techniques. Journal of Applied Polymer Science. 1993;**48**:2063-2252. DOI: 10.1002/app.1993.070481213

[26] Fieldson GT, Barbari TA. The use of FTIR-ATR spectroscopy to characterize penetrant diffusion in polymers. Polymer. 1993;**34**:1146-1156. DOI: 10.1016/0032-3861(93)90765-3

[27] Fieldson GT, Barbari TA. Analysis of diffusion in polymers using evanescent field spectroscopy. AICHE Journal. 1995;**41**:795-804. DOI: 10.1002/aic.690410406

[28] Nguyen T, Byrd E, Lin C. A spectroscopic technique for in situ measurement of water at the coating/metal interface. Journal of Adhesion Science and Technology. 1991;**5**:697-709. DOI: 10.1163/156856191X00648

[29] Philippe L, Lyon S, Sammon C, Yarwood J. An FTIR/ATR in situ study of sorption and transport in corrosion protective organic coatings: 1. Water sorption and the role of inhibitor anions. Progress in Organic Coating. 2004;**49**:302-314. DOI: 10.1016/j.porgcoat.2003.07.002

[30] Pereira MR, Yarwood J. ATR-FTIR spectroscopic studies of the structure and permeability of sulfonated poly(ether sulfone) membranes. Part 1. Interfacial water-polymer interactions. Journal of the Chemical Society, Faraday Transactions. 1996;**92**:2731-2735. DOI: 10.1039/FT9969202731

[31] Pereira MR, Yarwood J. ATR-FTIR spectroscopic studies of the structure and permeability of sulfonated poly(ether sulfone) membranes. Part 2. Water diffusion processes. Journal of the Chemical Society, Faraday Transactions. 1996;**93**:2737-2743. DOI: 10.1039/FT9969202737

[32] Hajatdoost S, Yarwood J. ATR-FTIR spectroscopic studies of the structure and permeability of sulfonated poly(ether sulfone) membranes. Part 3. Effects of sorption and desorption, and of annealing. Journal of the Chemical Society, Faraday Transactions. 1997;**93**: 1613-1620. DOI: 10.1039/A608447H

[33] Yarwood J, Sammon C, Mura C, Pereira MR. Vibrational spectroscopic studies of the diffusion and perturbation of water in polymeric membranes. Journal of Molecular Liquids. 1999;**80**:93-115. DOI: 10.1016/S0167-7322(99)80002-6

[34] Sammon C, Yarwood J, Everall N. A FTIR–ATR study of liquid diffusion processes in PET films: Comparison of water with simple alcohols. Polymer. 2000;**41**:2521-2534. DOI: 10.1016/S0032-3861(99)00405-X

[35] Wapner K, Stratmann M, Grundmeier G. In situ infrared spectroscopic and scanning Kelvin probe measurements of water and ion transport at polymer/metal interfaces. Electrochimica Acta. 2006;**51**:3303-3315. DOI: 10.1016/j.electacta.2005.09.024

[36] Wapner K, Grundmeier G. Spatially resolved measurements of the diffusion of water in a model adhesive/silicon lap joint using FTIR-transmission-microscopy. International Journal of Adhesion and Adhesives. 2004;**24**:193-200. DOI: 10.1016/j.ijadhadh.2003.09.008

[37] Nguyen T, Byrd E, Bentz D, Lin C. In situ measurement of water at the organic coating/substrate interface. Progress in Organic Coating. 1996;**27**:181-193. DOI: 10.1016/0300-9440(95)00535-8

[38] Baukh V, Huinink HP, Adan OCG, Sebastiaan J, Erich F, van der Ven LGJ. NMR imaging of water uptake in multilayer polymeric films: Stressing the role of mechanical stress. Macromolecules. 2010;**43**:3882-3889. DOI: 10.1021/ma1001996

[39] Bauer DR. Characterization of crosslinked polymers by high-resolution solids nuclear magnetic resonance spectroscopy. Progress in Organic Coating. 1986;**14**:45-65. DOI: 10.1016/0033-0655(86)80015-2

[40] Carr HY, Purcell EM. Effects of diffusion on free precession in nuclear magnetic resonance experiments. Physics Review. 1954;**94**:630-638. DOI: 10.1103/PhysRev.94.630

[41] Kimmich R, Fatkullin N. Polymer chain dynamics and NMR. Advances in Polymer Science. 2004;**170**:1-113. DOI: 10.1007/978-3-540-40000-4_5

[42] Adriaensens P, Pollaris A, Carleer R, Vanderzande D, Gelan J, Litvinov VM, et al. Quantitative magnetic resonance imaging study of water uptake by polyamide 4,6 (PA46) plates. Polymer. 2001;**42**:7943-7952. DOI: 10.1016/S0032-3861(01)00314-7

[43] Brownstein KR, Tarr CE. Importance of classical diffusion in NMR studies of water in biological cells. Physical Review A. 1979;**19**:2446-2453. DOI: 10.1103/PhysRevA.19.2446

[44] Araujo CD, Mackay AL, Whittall KP, Hailey JRT. A diffusion model for spin-spin relaxation of compartmentalized water in wood. Journal of Magnetic Resonance, Series B. 1993; **101**:248-261. DOI: 10.1006/jmrb.1993.1041

[45] Glover PM, Aptaker PS, Bowler JR, Ciampi E, McDonald PJ. A novel high-gradient permanent magnet for the profiling of planar films and coatings. Journal of Magnetic Resonance. 1999;**139**:90-97. DOI: 10.1006/jmre.1999.1772

[46] Aptaker PS, McDonald PJ, Mitchell J. Surface GARField: A novel one-sided NMR magnet and RF probe. Magnetic Resonance Imaging. 2007;**25**:548. DOI: 10.1016/j.mri.2007.01.020

[47] Zhu H, Huinink HP, Adan OCG, Kopinga K. NMR study of the microstructures and water-polymer interactions in cross-linked polyurethane coatings. Macromolecules. 2013; **46**:6124-6131. DOI: 10.1021/ma401256n

[48] Baukh V, Huinink HP, Adan OCG, Erich SJF, van der Ven LGJ. Water-polymer interactions during water. Macromolecules. 2011;**44**:4863-4871. DOI: 10.1021/ma102889u

[49] Federici JF. Review of moisture and liquid detection and mapping using terahertz imaging. Journal of Infrared, Millimeter and Terahertz Waves. 2012;**33**:97-126. DOI: 10.1007/s10762-011-9865-7

[50] Hu BB, Nuss MC. Imaging with terahertz waves. Optics Letters. 1995;**20**:1716-1718. DOI: 10.1364/OL.20.001716

[51] Mittleman DM, Jacobsen RH, Nuss MC. T-Ray imaging. IEEE Journal of Selected Topics in Quantum Electronics. 1996;**2**:679-692. DOI: 10.1109/2944.571768

[52] Jordens C, Wietzke S, Scheller M, Koch M. Investigation of the water absorption in polyamide and wood plastic composite by terahertz time-domain spectroscopy. Polymer Testing. 2010;**29**:209-2015. DOI: 10.1016/j.polymertesting.2009.04.010

[53] Stiens J et al. Enhanced Characterization of Dielectric Materials, EP15189446. 2015

[54] Pandey G. Ultra-sensitive millimeter wave sensor for material characterization [thesis]. Brussels, Belgium: Vrije Universiteit Brussel; 2017

[55] Pandey G, Vandermeiren W, Dimiccoli L, Stiens J. Contactless monitoring of food drying and freezing processes with millimeter waves. Journal of Food Engineering. 2018;**226**:1-8. DOI: 10.1016/j.jfoodeng.2018.01.003

[56] Pourkazemi A, Stiens JH, Becquaert M, Vanderwal M. Transient radar method: Novel illumination and blind electromagnetic/geometrical parameter extraction technique for multilayer structures. IEEE Transactions on Microwave Theory and Techniques. 2017;**65**: 2171-2184. DOI: 10.1109/TMTT.2017.2665633

[57] Obradovic J, Collins JHP, Hirsch O, Mantle MD, Johns ML, Gladden LF. The use of THz time-domain reflection measurements to investigate solvent diffusion in polymers. Polymer (Guildf). 2007;**48**:3494-3503. DOI: 10.1016/j.polymer.2007.04.010

[58] Kusano M, Kubouchi M, Bulgarevich DS, Shiwa M. Non-destructive evaluation by terahertz spectroscopy for penetration of acid solutions into epoxy resin. Express Polymer Letters. 2016;**10**:941-949. DOI: 10.3144/expresspolymlett.2016.87

[59] Deflorian F, Rossi S. An EIS study of ion diffusion through organic coatings. Electrochimica Acta. 2006;**51**:1736-1744. DOI: 10.1016/j.electacta.2005.02.145

[60] Castela ASL, Simões AM, Ferreira MGS. EIS evaluation of attached and free polymer films. Progress in Organic Coating. 2000;**38**:1-7. DOI: 10.1016/S0300-9440(99)00076-4

[61] Fredj N, Cohendoz S, Mallarino S, Feaugas X, Touzain S. Evidencing antagonist effects of water uptake and leaching processes in marine organic coatings by gravimetry and EIS. Progress in Organic Coating. 2010;**67**:287-295. DOI: 10.1016/j.porgcoat.2009.11.001

[62] Deflorian F, Fedrizzi L, Rossi S, Bonora PL. Organic coating capacitance measurement by EIS: Ideal and actual trends. Electrochimica Acta. 1999;**44**:4243-4249. DOI: 10.1016/S0013-4686(99)00139-5

[63] Brasher DM, Kingsbury AH. Electrical measurements in the study of immersed paint coatings on metal. I. Comparison between capacitance and gravimetric methods of estimating water-uptake. Journal of Applied Chemistry. 1954;**4**:62-72. DOI: 10.1002/jctb.5010040202

[64] Lindqvist SA. Theory of dielectric properties of heterogeneous substances applied to water in a paint film. Corrosion. 1985;**41**(2):69-75. DOI: 10.5006/1.3581974

[65] Galliano F, Landolt D. Evaluation of corrosion protection properties of additives for water-borne epoxy coatings on steel. Progress in Organic Coating. 2002;**44**:217-225. DOI: 10.1016/S0300-9440(02)00016-4

[66] Deflorian F, Fedrizzi L, Bonora PL. Influence of the photo-oxidative degradation on the water barrier and corrosion protection properties of polyester paints. Corrosion Science. 1996;**38**:1697-1708. DOI: 10.1016/S0010-938X(96)00062-5

[67] Bellucci F, Nicodemo L. Water transport in organic coatings. Corrosion. 1993;**49**:235-247. DOI: 10.5006/1.3316044

[68] Nguyen Dang D, Peraudeau B, Cohendoz S, Mallarino S, Feaugas X, Touzain S. Effect of mechanical stresses on epoxy coating ageing approached by electrochemical impedance spectroscopy measurements. Electrochimica Acta. 2014;**124**:80-89. DOI: 10.1016/j.electacta.2013.08.111

[69] Zhu H, Huinink HP, Erich SJ, Baukh V, Adan OC, Kopinga K. High spatial resolution NMR imaging of polymer layers on metallic substrates. Journal of Magnetic Resonance. 2011;**214**:227-236. DOI: 10.1016/j.jmr.2011.11.009

[70] Holtzman KA. Water vapor transport in adherent organic coatings. Journal of Paint Technology. 1971;**554**:47

[71] Rosen HN, Martin JM. Sorption of moisture on epoxy and alkyd free films and coated steel panels. Journal of Coatings Technology and Research. 1991;**63**:85